Micromagnetic simulation of 360° domain walls in thin Co films

T. Schrefl,[a] J. Fidler, and M. Zehetmayer
Institute für Angewandte und Technische Physik, Vienna University of Technology, Wiedner Hauptstrasse 8-10, A-1040 Vienna, Austria

A moving mesh finite element technique is applied to simulate the formation and annihilation of 360° wall structures in thin Co films. Adaptive refinement and coarsening of the finite element mesh controls the discretization error during the simulation of domain wall movement. Elements are refined in regions with high variation of the magnetization, whereas elements are taken out where the magnetization is uniform. The calculated Neel walls have very wide tails and have an extension of about 15–20 nm. The motion of domain walls through the sample gives rise to the formation of 360° domain walls. They are formed when a Bloch line in a domain wall is caught at a nonmagnetic defect in the sample. Pinholes with an extension greater than 6 nm are sufficient to trap a Bloch line. The width of the 360° walls is found to be in the range of 40 to 50 nm. The stability of the 360° walls depends on the strength of the pinning of the Bloch lines. The field required to annihilate the 360° walls increases linearly with the size of the nonmagnetic defect. © *2000 American Institute of Physics.* [S0021-8979(00)81608-4]

I. INTRODUCTION

The performance of magnetic sensors such as GMR multilayer films sensitively depends on the free motion of domain walls through the film. Structural inhomogeneities give rise to domain wall pinning and the formation of 360° walls. Such spiraling domain structures that are hard to annihilate deteriorate the sensitivity of the sensors. Heyderman and co-workers investigated the formation and annihilation of 360° domain walls in exchange coupled multilayer films using Fresnel imaging[1] and differential phase contrast microscopy.[2] In these multilayer films the easy direction magnetization reversal occurs by domain wall motion. As the domain walls move through the sample 360° wall structures are formed. The 360° wall structures were found to be stable up to high field values. Schäfer and Hubert[3] reported that 360° walls may act as nucleation sites for the magnetization process, observing domains and domain walls in sputtered exchange biased wedges. Again the elimination of the 360° wall structures was found to be strongly impeded. Berkov and co-workers[4] applied a micromagnetic model to investigate the formation and annihilation of 360° walls in antiferromagnetically coupled multilayers. The magnetization configuration near the end of linear defects was found to be crucial for the occurrence of 360° walls.

The stability of 360° wall structures is a common feature of very thin films. This phenomenon was originally investigated in classical transmission electron microscopy and Bitter pattern studies.[5] In thin films Neel walls decrease in energy and increase in width with decreasing film thickness.[6] Bloch lines within the Neel walls are easily caught by defects. The Bloch lines are pinned at nonmagnetic gaps in the film reducing the high exchange and stray field energy concentration of the Bloch line core. The Bloch line remains pinned, even if the walls generate nonequilibrium configurations as a consequence. A 360° wall is formed, if a 180° wall sweeps through the film, passes a pinhole, and a Bloch line gets caught.

In this article a newly developed adaptive finite element method[7] is used to simulate domain wall motion, Bloch line pinning, and the formation and annihilation of 360° walls in a Co thin film. In Sec. II of the article, we describe the micromagnetic finite element algorithm. In Sec. III we present a numerical simulation of the formation of 360° wall structures in thin Co films. In Sec. IV we summarize the results.

II. ADAPTIVE FINITE ELEMENT MICROMAGNETICS

The micromagnetic simulation of domain wall motion starts from the Gilbert equation,[8]

$$\frac{\partial \mathbf{J}}{\partial t} = -|\gamma|\mathbf{J}\times\mathbf{H}_{\text{eff}} + \frac{\alpha}{J_S}\mathbf{J}\times\frac{\partial \mathbf{J}}{\partial t}, \tag{1}$$

which describes the motion of the magnetic polarization vector $\mathbf{J}$ toward its equilibrium configuration. The effective field, $\mathbf{H}_{\text{eff}} = -\delta E_t/\delta \mathbf{J}$, is the variational derivative of the magnetic Gibb's free energy. A Gilbert damping constant $\alpha = 1$ was used. The total magnetic Gibb's free energy is the sum of the exchange energy, the magnetocrystalline anisotropy energy, the magnetostatic energy, and the Zeeman energy:[9]

$$E_t = \int \left(A\sum\nolimits_{i=1}^{3} (\nabla \beta_i)^2 + f_k(\mathbf{J}) - \frac{1}{2}\mathbf{J}\cdot\mathbf{H}_d - \mathbf{J}\cdot\mathbf{H}_{\text{ext}} \right) dV, \tag{2}$$

where β_1, β_2, β_3 denote the direction cosines of the magnetic polarization vector. A is the exchange constant and f_k is the energy density associated with a uniaxial magnetocrystalline anisotropy. $\mathbf{H}_d$ and $\mathbf{H}_{\text{ext}}$ denote the demagnetizing and the external field, respectively. In order to transform (1) into a system of ordinary differential equations, the box method[10] is used to approximate the effective field at the nodal points of the finite element mesh. The film is divided into tetrahe-

[a]Electronic mail: thomas.schrefl@tuwien.ac.at

TABLE I. Intrinsic magnetic properties used for the calculations. The uniaxial magnetocrystalline anisotropy constants K_1, the saturation polarization J_s, the exchange constant A, and the film thickness t.

K_1 (kJ/m^3)	J_s (T)	A (pJ/m)	t (nm)
450	1.76	13	1

dral finite elements. Within each element the direction cosines and a magnetic scalar potential U are interpolated by linear functions. The demagnetizing field $\mathbf{H}_d$ follows from the magnetic scalar potential, which is calculated using a hybrid finite element/boundary technique.[11] The resulting system of ordinary differential equations is integrated using explicit Runge–Kutta–Chebyshev formulas of order two. The algorithm[12] is appropriate for the solution to modest accuracy of a semistiff differential equation.

A coarse mesh may be sufficient in regions where the magnetization is almost uniform. Local mesh refinement near domain walls significantly reduces the number of degrees of freedom. As domain walls can move due to external fields the discretization has to be adjusted adaptively during the simulation. Refinement of the tetrahedral mesh at the current wall position and coarsening within the bulk of the domains leads to a high-density mesh that moves together with the wall.[7] The deviation of $|\mathbf{J}|$ from J_s within an element is used as an error indicator for the adaptive refinement schemes. Successive refinement of elements where $|\mathbf{J}|$ deviates from J_s leads to a fine mesh in areas with large spatial variation of the magnetization direction. In addition, finite elements whose error indicator is below a certain threshold can be taken out. After several refinement and coarsening steps the constraint $|\mathbf{J}| = J_s$ will be approximately fulfilled on the entire finite element mesh.

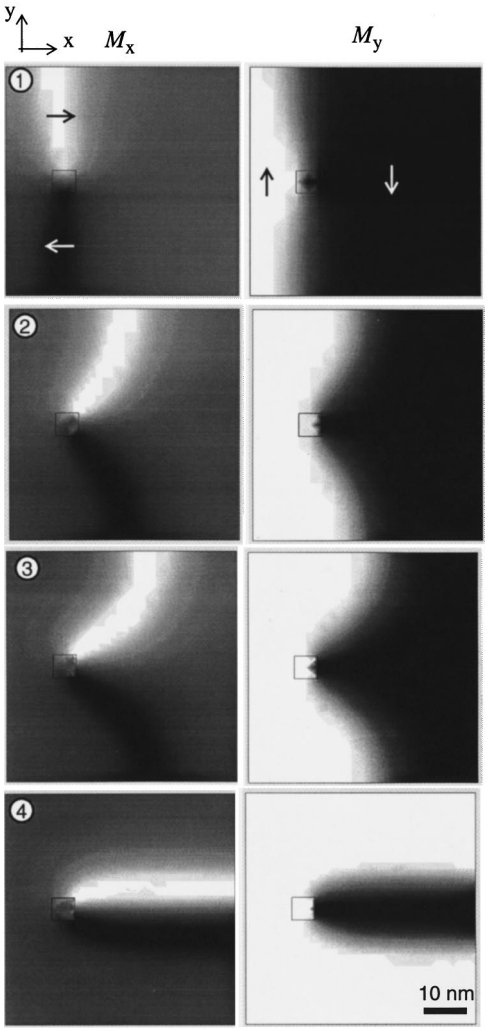

FIG. 1. Simulation of the formation of a 360° domain wall in a thin Co film. An external field of $H_{ext}=160$ kA/m is applied in the positive y direction. The gray scale plots of the left and right columns depict the x and y components of the magnetization, respectively. The numbers refer to the finite element grids presented in Fig. 2.

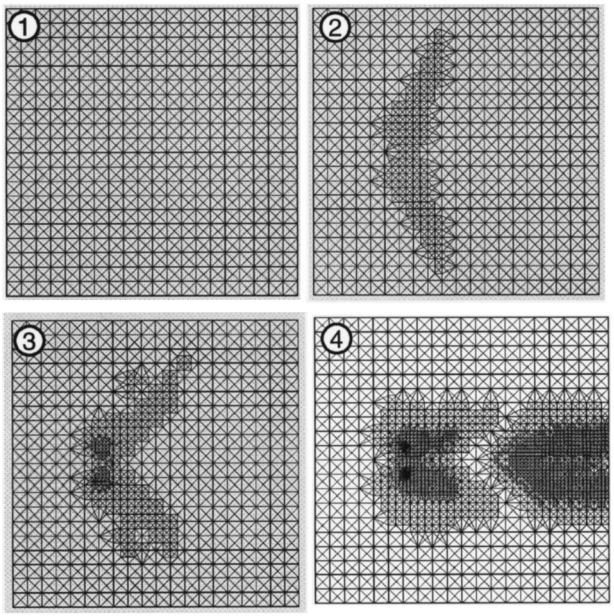

FIG. 2. The surface of the finite element mesh at different stages during adaptive refinement and coarsening.

III. RESULTS AND DISCUSSION

Table I shows the intrinsic magnetic properties used to simulate the interaction of a 180° domain wall with a nonmagnetic inclusion in a thin Co film with in-plane uniaxial anisotropy. The film thickness was 1 nm and the width of the quadratic defect was varied in the range of 6 to 12 nm. Figure 1 shows the motion of a 180° domain wall that interacts with a pinhole. The film has a thickness of only 1 nm. As a consequence, the Neel wall shows a wide tail. The wall width is about 15–20 nm. The wall moves to the right under the influence of an applied field of $H_{ext}=160$ kA/m. As the Bloch line gets caught at the nonmagnetic defect with an extension of 6 nm, a nonequilibrium wall configuration forms. In what follows, a horizontal 360° wall is generated.

Figure 2 gives the finite element grids at different stages during the formation of the 360° wall structure. The adaptive refinement and coarsening scheme leads to a fine grid in regions with high variation of the magnetization direction. Mesh 1 gives the initial grid. Mesh 2 and 3 show the finite elements at intermediate stages. The final mesh 4 is the result

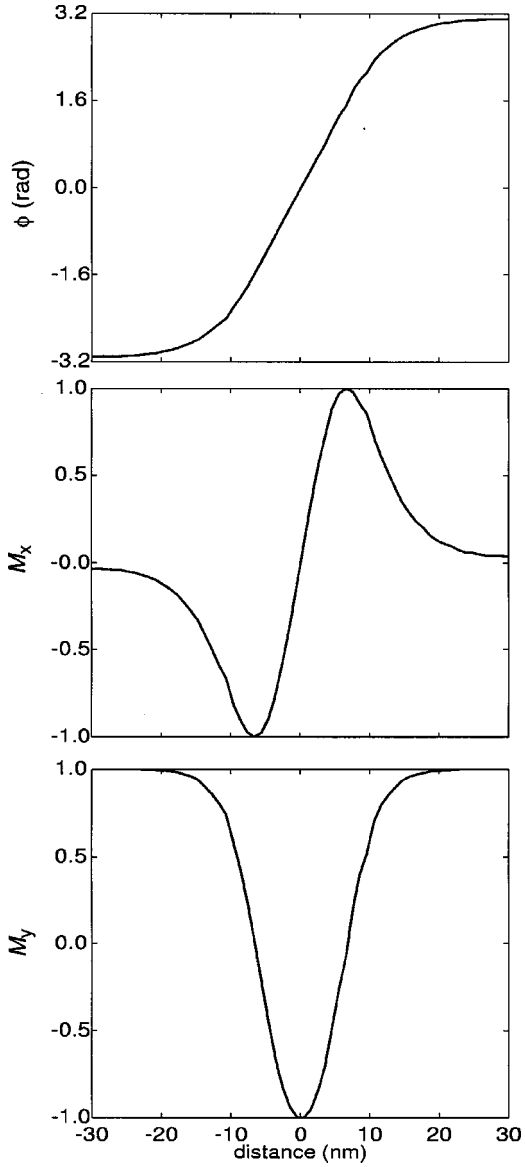

FIG. 3. Profile of the horizontal 360° wall. The plots give the angle of the magnetization with respect to the *y* axis, the *x* component of the magnetization, and the *y* component of the magnetization as a function of distance along a line parallel to the *y* axis.

of 20 refinement and coarsening steps. Within the framework of the refinement algorithm,[13] only elements that have been generated in the preceding refinement step can be taken out in a coarsening step. In addition, tangling nodes have to be avoided during the entire refinement and coarsening process. These constraints limit the set of possible finite element grids. As a consequence, the final mesh is not continuous in the center of the horizontal 360° wall. This restriction does not influence the final wall structure.

From Fig. 3, giving the wall profile, the width of the wall is estimated to be 40 nm. The field required to eliminate the 360° wall structure is calculated as a function of the defect size. The Bloch line remains pinned at the nonmagnetic gap in high external fields. Figure 4 shows the field required to depin the Bloch line as a function of the defect size. Fields in the range from 240 to 300 kA/m are necessary to eliminate the 360° wall structure for a defect size ranging from 6 to 12 nm, respectively.

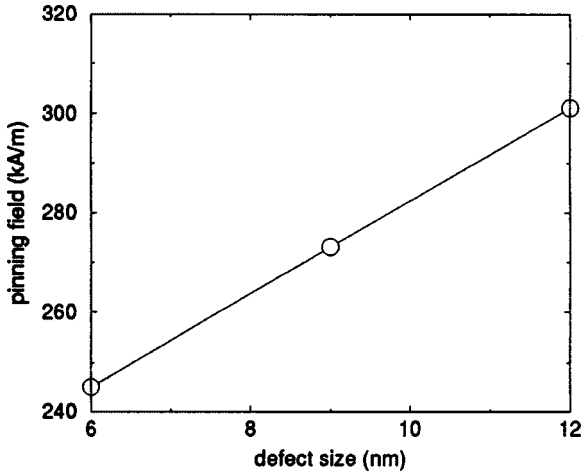

FIG. 4. The external field required to eliminate the 360° wall structure as a function of the size of the nonmagnetic defect.

IV. CONCLUSIONS

In this paper a novel finite element refinement technique has been applied to simulate the formation and annihilation of 360° degree wall structures in very thin Co films with in-plane magnetocrystalline anisotropy. The refinement and coarsening scheme refines the finite element mesh at the current wall position during the simulation of wall motion. As the wall sweeps through the film nonmagnetic defects may pin a Bloch line, causing the formation of a 360° wall structure. In order to eliminate the 360° wall, an external field of 280 kA/m is required for a defect size of 10 nm.

ACKNOWLEDGMENT

This work was supported by the Austrian Science Fund (Projects No. 13260 TEC and No. Y132-PHY).

[1] L. J. Heyderman, J. N. Chapman, and S. S. P. Parkin, J. Magn. Magn. Mater. **138**, 344 (1994).
[2] L. J. Heyderman, J. N. Chapman, and S. S. P. Parkin, J. Appl. Phys. **76**, 6613 (1994).
[3] R. Schäfer and A. Hubert, IEEE Trans. Magn. **29**, 2738 (1993).
[4] D. V. Berkov, N. L. Gorn, R. Mattheis, and T. Zimmermann, J. Magn. Magn. Mater. **182**, 81 (1998).
[5] E. Feldtkeller and W. Liesk, Z. Angew. Phys. **14**, 195 (1962).
[6] A. Hubert and R. Schäfer, *Magnetic Domains* (Springer, Berlin, 1998).
[7] W. Scholz, T. Schrefl, and J. Fidler, J. Magn. Magn. Mater. **196–197**, 933 (1999).
[8] T. L. Gilbert, Phys. Rev. **100**, 1243 (1955).
[9] W. F. Brown, Jr., *Micromagnetics* (Wiley, New York, 1963).
[10] W. Hackbusch, Computing, Archives for Scientific Computing **41**, 277 (1989).
[11] D. R. Fredkin and T. R. Koehler, IEEE Trans. Magn. **26**, 415 (1990).
[12] B. P. Sommeijer, L. F. Shampine, and J. G. Venwer, J. Comput. Appl. Math. **66**, 315 (1998).
[13] J. Bey, Computing **55**, 355 (1995).